Electron spin resonance study of atomic hydrogen stabilized in solid neon below 1 K.

S. Sheludiakov,* J. Ahokas, J. Järvinen, L. Lehtonen, and S. Vasiliev†
Department of Physics and Astronomy, University of Turku, 20014 Turku, Finland

Yu. A. Dmitriev
Ioffe Institute RAS, 26 Politekhnicheskaya, St. Petersburg 194021, Russian Federation

D. M. Lee and V. V. Khmelenko
Institute for Quantum Science and Engineering, Department of Physics and Astronomy, Texas A&M University, College Station, TX, 77843, USA

(Dated: March 9, 2018)

We report on an electron spin resonance study of atomic hydrogen stabilized in solid Ne matrices carried out at a high field of 4.6 T and temperatures below 1 K. The films of Ne, slowly deposited on the substrate at the temperature ∼1 K, exhibited a high degree of porosity. We found that H atoms may be trapped in two different substitutional positions in the Ne lattice as well as inside clusters of pure molecular H_2 in the pores of the Ne film. The latter type of atoms was very unstable against recombination at temperatures 0.3-0.6 K. Based on the observed nearly instant decays after rapid small increases of temperature, we evaluate the lower limit of the recombination rate constant $k_r \geq 5 \cdot 10^{-20}\,\mathrm{cm^3 s^{-1}}$ at 0.6 K, five orders of magnitude larger than that previously found in the thin films of pure H_2 at the same temperature. Such behavior assumes a very high mobility of atoms and may indicate a solid-to-liquid transition for H_2 clusters of certain sizes, similar to that observed in experiments with H_2 clusters inside helium droplets (Phys. Rev. Lett 101, 205301 (2008)). We found that the efficiency of dissociation of H_2 in neon films is enhanced by 2 orders of magnitude compared to that in pure H_2 as a result of strong action of secondary electrons.

I. INTRODUCTION

Quantum properties of insulating solids are most pronounced for molecular and atomic crystals of the lightest elements H_2, He, Ne. While making a solid from helium requires applying high pressure even at zero temperature, hydrogen and neon solidify at ambient pressure and fairly high temperatures. These solids may serve as matrices for stabilizing unstable and highly reactive species and radicals. Being introduced into an inert solid matrix, these species become immobilized and remain stable at low enough temperatures where their diffusion is suppressed. Matrices made out of mixtures of neon and hydrogen are most intriguing because the Lennard-Jones potential parameters for the H_2-H_2 and H_2-Ne pairwise interaction are nearly identical [1] while a large difference of their masses allows considering H_2 and Ne as isotopes of the same substance with an astonishingly different degree of quantumness.

The solid solutions of H_2-Ne may form various interesting phases. It turns out that the equilibrium solubility of H_2 in solid neon is vanishingly small and does not exceed a fraction of a percent for films crystallized from liquids. However, the situation is different for the non-equilibrium samples prepared by rapid flash-condensing of the films. Such non-equilibrium samples may contain a co-existing metastable *hcp* phase of solid Ne along with the *fcc* and *hcp* structures of Ne and H_2, respectively [1]. The phases of molecular hydrogen appear in the form of nanocluster inside solid neon already at concentrations as low as 0.01% [2]. Solid rare-gas films quench-condensed on a cold substrate were found to be highly disordered and porous [3].

The possibility of formation of small hydrogen clusters in neon crystals has another important consequence, since it has been predicted that in a restricted geometry the freezing temperature may be substantially lowered and one may supercool liquid hydrogen to the superfluid transition, which may occur at a temperature of ∼6 K [4]. The liquid-like behavior of hydrogen clusters surrounded by superfluid helium film has been reported for clusters composed of $\sim 10^4$ molecules at a temperature of ∼1 K [5], and for small clusters of less than 30 molecules, a superfluid response was predicted [6–8] and observed at 0.15 K [9]. This observation, however, was somewhat controversial [10, 11] resulting in an uncertainty for the behavior of clusters of intermediate size.

Hydrogen atoms can be obtained inside solid matrices by dissociation of molecular H_2 using e.g. electrons or γ-rays. Due to their small size, H atoms may occupy different lattice positions in the matrix where their interaction with the host particles may slightly change both their electronic g-factors and the hyperfine constants as compared with those of free atoms in the gas phase [12]. The weak interatomic van-der-Waals attractive interaction, Ne-Ne, can be easily overcome if the H atom is introduced into an interstitial position of the neon matrix. In this case, a strong Ne-H repulsion which appears at short

* Present address: Institute for Quantum Science and Engineering, Department of Physics and Astronomy, Texas A&M University, College Station, TX, 77843, USA
† servas@utu.fi

distances rearranges the host atoms around the hydrogen guests in a way such that the H atoms finally reside in the substitutional positions. This process, known as relaxation [13], also takes place in the matrices of solid hydrogen isotopes where a strong H-H_2 repulsion does not allow stabilizing H atoms in the interstitial sites [14]. Relaxation of H atoms in the rare-gas solids was considered by Kiljunen et al. [15] who calculated that H atoms in solid Ne will reside in the substitutional positions regardless of their initial trapping sites.

Exposing solidified rare gases to an electron beam results in large yields of secondary electrons, as well as atomic and molecular excitons [16]. This is in stark difference to molecular solids, such as H_2 and D_2, where primary electrons can lose their energy by exciting rotational and vibrational transitions or by dissociating molecules [17]. The large quantity of secondary electrons is very effective for increasing the dissociation efficiency of H_2 molecules embedded in rare-gas matrices.

Stabilization of hydrogen atoms in solid neon has a long and controversial history. The first attempts to stabilize H atoms by co-deposition of the rf discharge products onto a cold substrate appeared to be unsuccessful, where only a single ESR line doublet was observed after *in situ* photolysis of HI [18]. This ESR line doublet was characterized by a positive hyperfine constant change, $\frac{\Delta A}{A} = 0.43\%$, and was attributed to the H atoms in the somewhat distorted substitutional positions of the Ne matrix. Later Zhitnikov and Dmitriev used a co-deposition technique and reported the observation of an extremely narrow, ∼80 mG wide, ESR line doublet with a negative hyperfine constant change $\frac{\Delta A}{A} = -0.1\%$ [2] which they attributed to H atoms in substitutional sites of an unperturbed solid Ne lattice. In a following work [19], Dmitriev et al. reported on the observation of two positions for H atoms in solid Ne characterized by both positive and negative hyperfine constant changes respectively. Along with a single positively shifted ESR line doublet of isolated atoms in solid Ne, Knight et al. and Correnti et. al. observed the ESR spectra of H-H and H-D radical pairs [20] and also H_2^+ ions [21] unstable in a hydrogen environment, respectively, using the same co-deposition technique.

In this work, we report on the first ESR study of atomic hydrogen trapped in solid Ne carried out in a high magnetic field (4.6 T) and at temperatures below 1 K. We found that the as-deposited Ne samples are highly disordered and porous, although the porosity can be significantly reduced by annealing the films at 7-10 K. The H_2 molecules in solid Ne were dissociated *in situ* by electrons released during the β-decay of tritium trapped in the metal walls of our sample cell. The accumulation rate of H atoms from dissociation of H_2 molecules in solid neon turned out to be enhanced by two orders of magnitude as compared with that in pure H_2. We attribute this to dissociation of H_2 molecules by secondary electrons released from neon atoms during the course of their bombardment by primary electrons generated in the β-decay of tritium. The ESR lines of H atoms in the as-deposited solid neon films had a complex shape which can be fitted by a sum of three peaks. These components were assigned to H atoms in different positions in the matrix, two of which correspond to the substitutional positions in the Ne lattice, while the third originates from the H atoms trapped in the regions of pure H_2. We found that raising the sample cell temperature from 0.1 K to 0.3-0.6 K leads to an abrupt recombination of the atoms inside regions of pure H_2. Such rapid recombination cannot occur at 0.6 K inside a solid. We will consider possibilities for the explanation of this effect.

II. EXPERIMENTAL DETAILS

The experiments were carried out in the sample cell (SC) shown in Fig. 1 [22]. The cell is attached to the mixing chamber of an Oxford 2000 dilution refrigerator to provide cooling. The minimum temperature attained in this set of experiments was ≃90 mK. The solid neon samples were deposited directly from a room temperature gas handling system at a deposition rate of 1-2 monolayers/s. We used a 99.99 % pure neon gas and did not add H_2 intentionally while we prepared so-called "pure" Ne samples. The mass-spectrometry analysis of the neon gas we used showed a H_2 content ≈100 ppm. The samples were deposited onto the top electrode of a quartz-crystal microbalance (QM) which has a mass resolution of about 0.02 Ne monolayer. The sample cell temperature during the film deposition was stabilized at 0.8-1.3 K. Prior to deposition, a small (∼mmol) amount of helium was condensed into a volume under the QM (see Fig. 1) for removing heat released during the film growth. The top electrode of the quartz microbalance is electrically insulated from the sample cell body which made it possible to apply electric potentials to the film substrate.

The QM top electrode also serves as a flat mirror of the ESR Fabry-Perot resonator. This allows a simultaneous measurement of the film thickness and ESR detection of the species in the film which possess unpaired electron spins. The main investigation tool in our work is a 128 GHz super-heterodyne ESR spectrometer which enables a simultaneous measurement of the real and imaginary components of rf magnetic susceptibility [23]. We will present only the ESR absorption spectra throughout the article. The spectrometer has a sensitivity of about 10^{11} spins at the excitation power of the order of 1 pW, while the maximum ESR excitation power available is of the order of 1 μW. The measurement of the H atom hyperfine constants was carried out by the method of electron-nuclear double resonance (ENDOR) which allows determination of the NMR transition frequency indirectly, by its influence on the ESR signal amplitude [24]. An auxiliary rf resonator (H NMR coil in Fig. 1) for performing ENDOR was arranged close to the top electrode of the quartz microbalance. The resonator was used to excite the $a-b$ NMR transition of hydrogen atoms

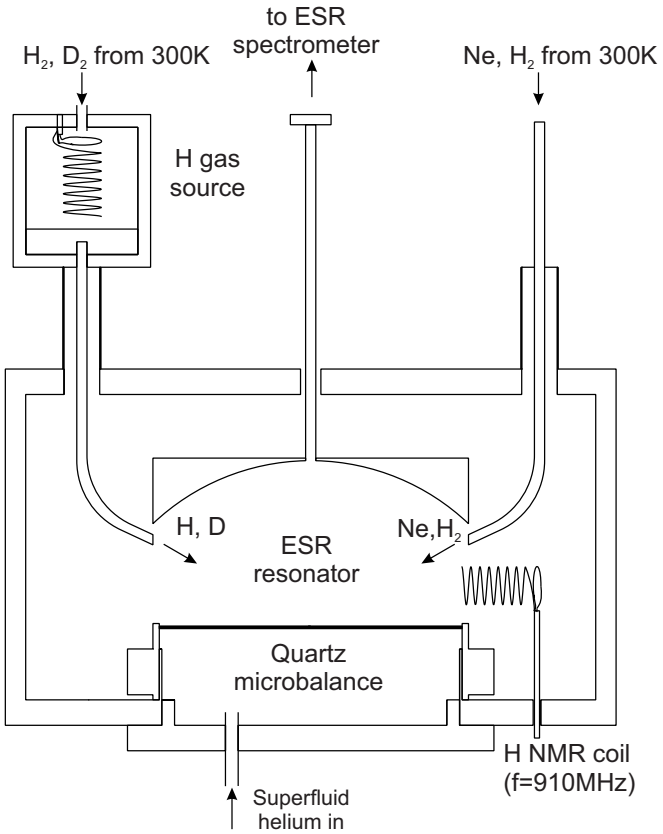

Figure 1. Sample cell schematic. The auxiliary rf resonator used for ENDOR is labeled as H NMR coil.

($f = 910\,\mathrm{MHz}$) (Fig. 2).

Construction of the sample cell also allows accumulation of H and D atoms in the gas phase at low densities. Recording ESR spectra from these atoms provides a reference for measurements of the ESR spectrum parameters of matrix isolated atoms by measuring the shifts of the ESR lines from positions of the lines of the gas-phase atoms. For filling the sample cell with hydrogen gas we use a cryogenic source of atoms (H-gas source) [25, 26] (a separate chamber located ~ 10 cm above the sample cell). Small amounts of molecular hydrogen are condensed into the H-gas source, and then the molecules are dissociated by running the RF discharge in a miniature coil inside the source. In order to suppress surface adsorption and recombination of atoms, the walls of the chamber are covered by a film of superfluid helium.

III. EXPERIMENTAL RESULTS

This work follows our previous study of unpaired atoms of hydrogen isotopes in solid films containing tritium [27]. Electrons with average energy of 5.7 keV resulting from tritium β-decay serve as an effective source of atoms due to *in situ* dissociation of molecules in the matrix. It turned out that in the course of previous experiments, substantial numbers of tritium atoms and molecules became trapped in the ESR resonator mirrors and possibly in the copper walls of the sample cell. We found that even warming the sample cell to room temperature and pumping it to high vacuum for several days does not completely remove tritium from the walls of the chamber. From the efficiency of production of stabilized H atoms we estimate that $\sim 10^{15}$ tritium atoms still remained trapped in the walls of the sample cell after cooling it to low temperatures.

Our original idea for studying neon was to cover the flat mirror of the ESR resonator by an inert absorptive layer which would capture electrons resulting from the decay of trapped tritium. Already in the first experiment with so-called "pure" (99.99%) solid neon films, we noticed an unexpectedly high accumulation rate of H atoms, $d[\mathrm{H}]/dt$, resulting from dissociation of trace amounts of H_2 molecules condensed with the neon gas. The ESR signal from H atoms in this neon film was only 20 times smaller than for H atoms trapped in a pure H_2 film of the same thickness. Followed by that, we carried out a series of experiments with solid neon-hydrogen samples with different admixtures of H_2, both as-deposited and annealed. We studied the following samples: a "pure" Ne film (Sample 1), Ne:0.2% H_2 (Sample 2), Ne:1% H_2 (Sample 3), Ne:3% H_2 (Sample 4), Ne:6% H_2 (Sample 5). Sample 6 was a "pure" Ne film, first studied as-deposited and then annealed and later a 160 nm pure H_2 film was deposited on top of it. All neon films had a thickness of 2.5 μm. We also studied a pure normal H_2 sample of the same thickness for the sake of comparison (Sample 7).

A typical experimental cycle included the following stages: deposition of the sample at the sample cell temperature 0.7-1.3 K, cooling down to the lowest temperature $\approx$0.1 K, waiting for 1-3 days for accumulation of the atoms in the deposited film. After that we usually condensed a small amount of ^{4}He into the sample cell in order to accumulate atoms in the gas phase and make accurate measurement of the spectroscopic parameters of H atoms in the matrix with respect to that of the free atoms. It turned out that admission of helium influenced properties of the samples substantially, which could be related to the overheating of the sample cell to 0.6 K during condensation. Therefore, for some samples prior to the film condensing, we performed a brief test of the sample reaction during the increase of temperature to 0.6 K.

It turned out that all as-deposited samples absorbed a substantial amount of helium, which indicated the high porosity of the films. In order to eliminate this, we performed annealing of the films by heating them to the temperatures of 7-9 K for 1-2 hours. This procedure was performed close to the end of the experimental cycle before destroying the sample.

ESR spectra of all visible components within $\pm$500 G from the H doublet center were periodically recorded at all stages of the experimental cycle. ENDOR studies were usually performed after the build up of strong enough

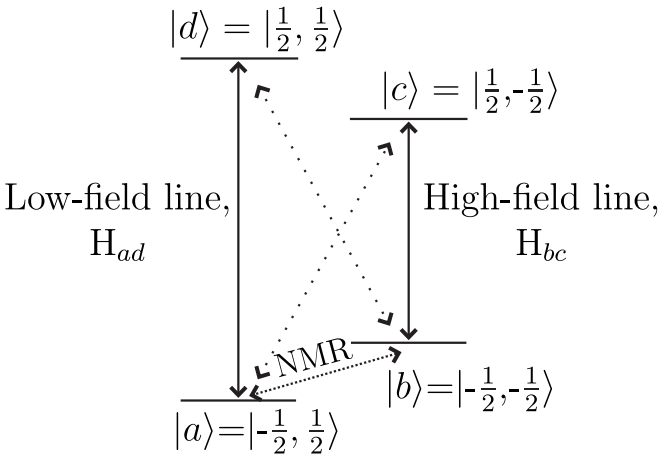

Figure 2. Energy level diagram of H atom in magnetic field. Solid arrows mark the allowed ESR transitions, dotted arrows - the forbidden transitions corresponding to a simultaneous spin flip of electron (S) and proton (I). The spin states are labeled as $|m_S, m_I\rangle$.

ESR signals of the H atoms.

Usually it took about 2 days to accumulate sufficiently strong ESR lines in "pure" neon samples, while the H atom ESR lines in Samples with 1% and higher H_2 admixture appeared within a few hours.

A. ESR spectra

The ESR lines of the H doublet had a complex shape, which is demonstrated in Figs. 3 and 4. Analyzing the H_{bc} lines we found that the best result is obtained by fitting them with 3 Lorentzian peaks slightly shifted from each other. In contrast, the H_{ad} lines had a much more regular, nearly Lorentzian shape. It would be impossible to analyse these complicated lineshapes with the ESR technique alone. However, thanks to two other magnetic resonance techniques: the Dynamic Nuclear Polarization (DNP) and Electron-Nuclear Double Resonance (ENDOR) we were able to make unambiguous conclusion about the ESR lines structure and its origin. Using the DNP and ENDOR, as described in the next section, we were able to figure out that there exists three distinct magnetic resonance transitions corresponding to different environments and locations of the H atoms in the lattice. Then, knowing that there are three transitions we used the ESR spectra for accurate measurements of their corresponding spectroscopic parameters.

The interaction of the guest H atoms with the host particles is expected to slightly change both their electronic g-factors and the hyperfine constants A compared to those of free atoms in the gas phase. The sign of a hyperfine constant change characterizes the lattice sites the H atoms occupy. It is negative for spacious substitutional positions and positive for more cramped interstitial sites [12]. Atoms in each position produce components in the ESR spectrum with different separations between the lines of the H doublet defined by the value of A, and different positions of the doublet center defined by the corresponding g-factors. It turns out that the components with larger A (Component 3 in Fig. 3) have a smaller g-factor and the center of the doublet is shifted to the right, towards a higher sweep field. Therefore, these contributions nearly compensate each other for the H_{ad} line and the different components appear almost merged, while they diverge for the H_{bc} line, where both the hyperfine constant and g-factor change increase the line shifts.

In addition to the lines of H atoms, we also observed two singlet lines close to the center of the ESR spectrum with g=2.00208 and g=2.00234 which we attributed to electrons trapped in solid neon and hydrogen rich regions (Fig. 5). Similar lines with g-factors nearly equal to that of free electrons were observed previously in different matrices of hydrogen isotopes [28, 29].

The shape of all ESR lines of H atoms in the different Ne:H_2 films we studied had a somewhat similar structure as shown in Fig. 4. The spectra were measured after 1.5-2 days of sample storage at T=90 mK. Fitting of the ESR lines of atomic hydrogen in neon for Sample 3 (Ne:1% H_2) by three Lorentzian lines is presented in Fig. 3. In order to make the fitting, we carefully measured the electronic g-factors of the H_{bc} line components using the reference line of free hydrogen atoms in the gas phase. The values of the hyperfine constants, A, for H atom doublets were measured using the ENDOR technique as described further. The positions of all three components of the H_{ad} line as shown in Fig. 3 were calculated based on the g-factors extracted for the H_{bc} line as well as measurement of the hyperfine constant by ENDOR, and the fitting was carried out having the component amplitudes as the only adjustable parameters. The values of A measured by ENDOR for different samples were nearly similar within the uncertainty (a few hundreds kHz), associated with the width of the observed ENDOR transitions. Therefore, we only present the spectroscopic parameters for H atom ESR line components for intermediate Sample 3 (Table I). The width of Components 1 and 2 increased in the samples with a high (3 and 6%) H_2 admixture which might be a result of their partial merging.

B. ENDOR

While the positions of the ESR lines depend on the values of the hyperfine constant A and the g-factor, which are slightly different for the atoms in different environments, the frequency of the pure NMR transition $a-b$ is mainly determined by the hyperfine constant. Due to the relatively poor sensitivity of NMR we cannot detect directly the $a-b$ transition by the conventional methods of NMR spectroscopy. Instead, the double resonance technique (ENDOR) utilizing simultaneous excitation of the electron and nuclear magnetic resonance transitions was used. The ENDOR method is based on determination

Present work						
	C1	C2	C3	H in H_2	e^- in Ne	e^- in H_2 clusters
g_e	2.00229(2)	2.00223(2)	2.00222(2)	2.00229(1)	2.00208	2.00234
A (MHz)	1417.7(4)	1419.0(3)	1426.2(5)	1417.40(2)		
ΔA (MHz)	-2.7(4)	-1.4(3)	5.8(5)	3.01(2)		
$\Delta A/A$ (%)	-0.19(3)	-0.10(2)	+0.40(3)	-0.21(1)		
Width (G)	0.8	1.3	1.8	1.0	2.1	0.6
Previous studies						
	C1	C2	C3	C1	C2	C3
g_e				2.00213(8)	2.00211(8)	2.00207(8)
A (MHz)	1417.4(2)	1418.99(15)	1426.11(15)	1417.4(2)	1418.5(3)	1426.56(20)
ΔA (MHz)	-3.0(2)	-1.42(15)	5.70(15)	-3.0(2)	-1.9(3)	6.15(20)
$\Delta A/A$ (%)	-0.21(1)	-0.10(1)	0.40(1)	-0.21(1)	-0.13(2)	0.43(1)
Width (G)		0.09	0.15-0.30	0.5	0.09	
Ref.	[19]			[2]		[18]

Table I. The main spectroscopic parameters measured for H atoms and electrons in Sample 3 (Ne:1% H_2) and Sample 7 (pure H_2) of the present work and those for H atoms in solid neon observed in previous studies [2, 18, 19].

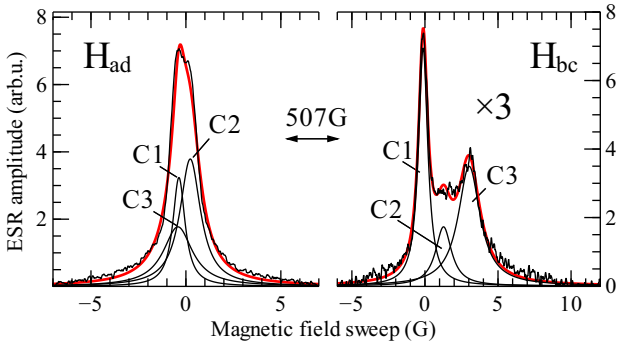

Figure 3. ESR spectra of atomic hydrogen in Sample 3 (Ne:1%H_2) after 2 days of storage. The H_{bc} and H_{ad} lines are fitted by three Lorentzian curves with parameters shown in Table I. The H_{bc} line amplitude is multiplied by a factor of 3.

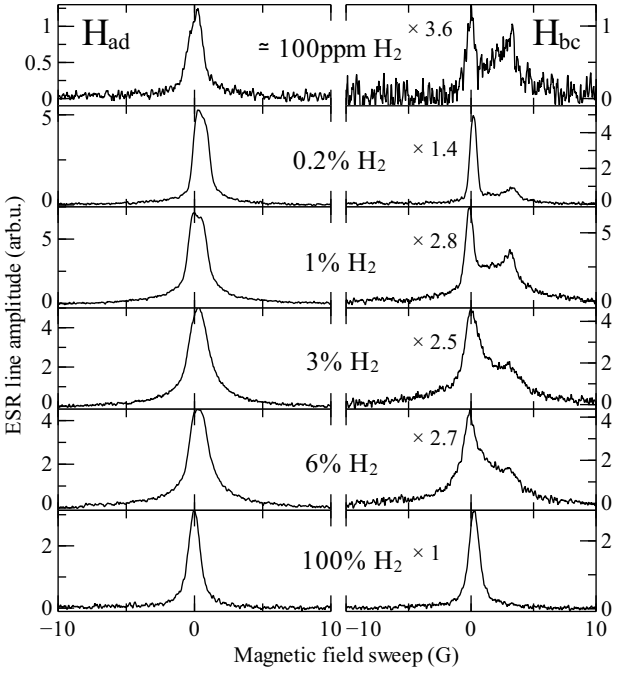

Figure 4. The H_{ad} and H_{bc} ESR lines measured in neon samples with different admixtures of H_2 studied in this work. Note that the H_{bc} line amplitudes are multiplied by a factor specified for each plot. The distance between the lines is ≃507 G.

of the NMR transition frequency indirectly by its influence on the ESR line amplitude when the rf excitation frequency exactly matches the $a-b$ transition frequency (see Fig. 2).

Prior to measuring ENDOR transitions, we created a Dynamic Nuclear Polarization (DNP) using the Overhauser effect [31] in order to decrease the H_b level population and enhance the ENDOR signal. The DNP procedure is based on saturation of the allowed ESR $b-c$ transition with a subsequent cross-relaxation via the forbidden $c-a$ transition (Fig. 2). Using this DNP method we were able to transfer all three components of the H_{bc} line to the H_{ad} line separately or transfer the whole line using 15 MHz FM modulation of the ESR spectrometer frequency. Relaxation of the hyperfine level populations is extremely slow at temperatures below 0.5 K. The non-equillibrium spin distribution created by such DNP stays unchanged for a long time, sufficient for making the ENDOR measurements.

The ENDOR spectroscopy was performed by two slightly different procedures. We applied RF excitation to the H NMR coil (Fig. 1) at the frequency f_{NMR} close to that of the NMR transition for free H atoms ($f_{ab} \approx$

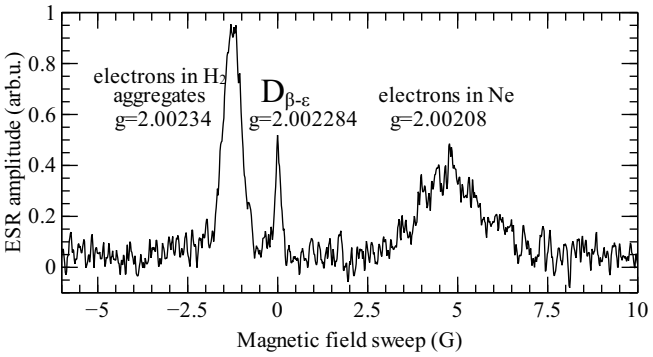

Figure 5. Magnified center of the ESR spectrum measured in Sample 1 (a "pure" Ne film) after condensing helium film into the sample cell and accumulating signal of deuterium atoms in the gas phase. The $D_{\beta-\epsilon}$ line of free D atoms in the gas phase (g=2.002284 [30]) was used as a magnetic field reference for determining the g-factors of other ESR lines in the figure (Table I). See Page 8 for a detailed discussion.

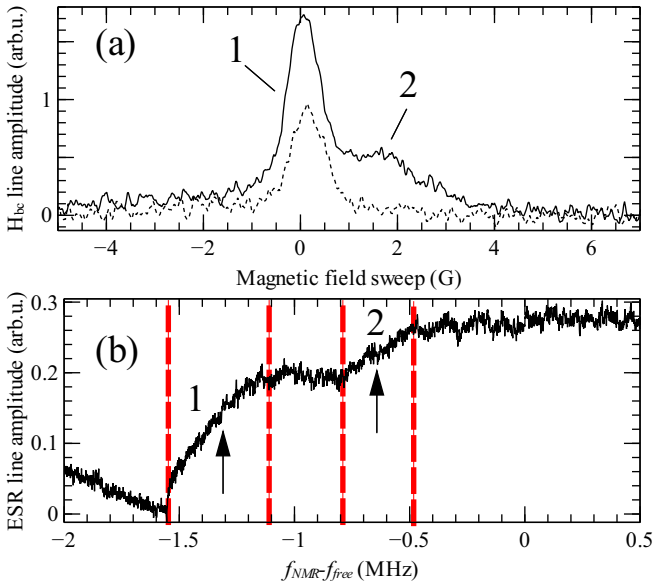

Figure 6. H_{bc} line before (dashed) and after (solid) measuring ENDOR spectrum (a). ENDOR spectrum showing transitions recovering the first (C1) and second (C2) component of the H_{bc} line measured in Sample 6 (Ne/H_2) (b). Note that only Components 1 and 2 in (a) increased. The ENDOR transitions margins are designated by red dashed lines. The resonance positions for each transition are marked by arrows.

910 MHz). In order to cover some frequency range with this excitation we used small (several tens of kHz) frequency modulation around the average frequency value. Pumping at different values of the f_{NMR} for several tens of minutes we checked effect on the amplitudes of the H_{bc} lines. Scanning the region $\pm$5 MHz around the resonance value for free atoms, we were able to identify three distinct regions where, as a result of pumping, one of the components of the H_{bc} has recovered. Such scanning allows rough determination of the transition margins with certain constraints on their width.

Actual ENDOR spectra were detected by a second method. Stopping the magnetic field sweep at the position of one of the components (C_1, C_2 and C_3) of the H_{bc} ESR line, we performed slow scans of the f_{NMR}. By recording the ESR signal recovery as a function of the applied RF frequency we retrieved the ENDOR spectra for each component of the H_{bc} line. The ENDOR spectra recorded by this method are presented in Figs. 6b and 7b. Despite the relatively large width of the NMR transitions and poor signal-to-noise ratio of the ENDOR spectra, utilizing these two methods in multiple measurements for different samples provided reproducible results for all three transitions. Figs. 6b and 7b show the regions (1, 2 and 3) where the H_{bc} line amplitudes increased during passage through the corresponding NMR transitions. Vertical dashed lines designate the beginnings and ends of the NMR transitions for different components of the H_{bc} line (C_1, C_2 and C_3). The arrows show the positions of resonances for the NMR transitions, which we used for the determination of the corresponding hyperfine constants.

Pumping the H_{bc} line without modulation burned a 0.1 G wide hole in the H_{bc} line which was reproducible for all three components. The hole formation corresponds to saturation of an individual group of spins and its width provides a contribution from homogeneous broadening which is determined by the dipolar interaction between the electron spins of atoms.

The hyperfine constant can be determined from the measured transition frequency according to the formula [32]

$$A \simeq 2f_{NMR} - \frac{\gamma_H B}{\pi} \qquad (1)$$

where γ_H is the proton gyromagnetic ratio and B is the static magnetic field. We found that the ESR lines were easily saturated which made the registration of ENDOR spectra rather difficult. In the Figs. 6 and 7, we present the ENDOR spectra measured for Sample 6 (Ne/H_2) where they appeared to be unambiguous and clear. The ENDOR transition widths are solely defined by the spread of hyperfine constants A for each component. Therefore, we constrain the uncertainty of determining A for each component by the width of a corresponding ENDOR transition. The spectroscopic parameters for Samples 1-6 coincided within the experimental uncertainty. Therefore, we present in Table I only the values of A and g for an intermediate Sample 3, Ne:1%H_2.

Recovering the ESR line components after pumping the NMR transitions confirms the determination of their frequencies performed by ENDOR. The first two ENDOR transitions are shown in Fig. 6. Transitions 1 and 2 recovered the left (C1) and the central components (C2) of the H_{bc} line, respectively. The first transition corresponds to a hyperfine constant change of -2.6(4) MHz.

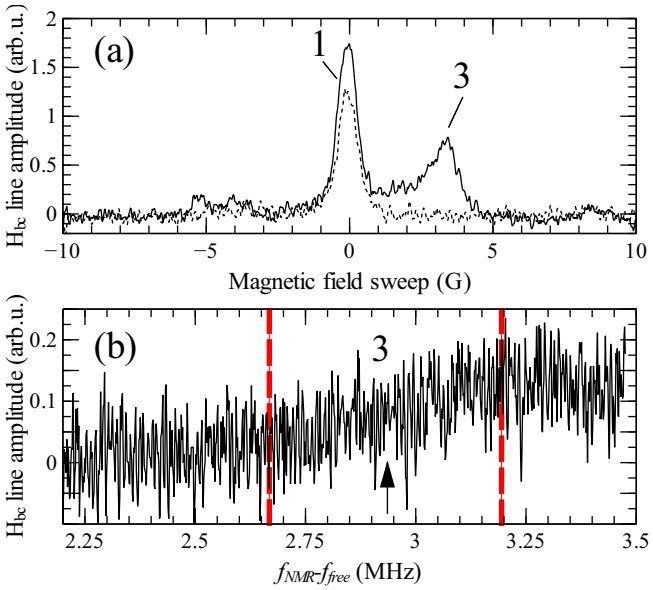

Figure 7. H_{bc} line before (dashed) and after (solid) measuring ENDOR spectrum (a). ENDOR spectrum recovering the third (C3) H_{bc} line component measured in Sample 6 (Ne/H_2) (b). Note that only Component 3 in (a) increased. The small increase of Component 1 is due to the relaxation process. The transition margins are designated by red dashed lines The resonance position is marked by arrow.

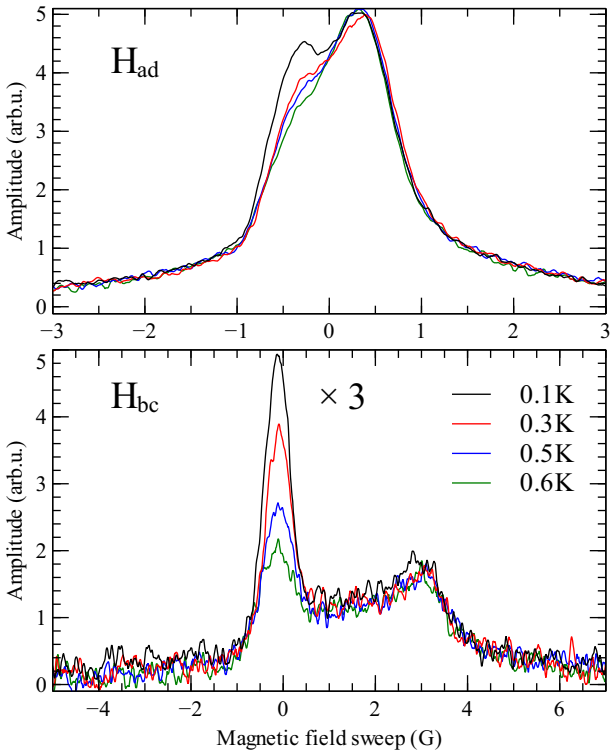

Figure 8. Effect of step-wise raising temperature in the range from 0.1 to 0.6 K on ESR lines of H atoms in Sample 3 (Ne:1%H_2). Note that only the left peak corresponding to Component 1 in both lines changes. Note that the H_{bc} line amplitude is multiplied by a factor of 3.

The second transition corresponds to a smaller hyperfine constant shift, ΔA=−1.4(3) MHz. Both transitions, 1 and 2, are characterized by negative hyperfine constant changes and can be attributed to the substitutional positions in the matrix [12]. The second transition appeared only in Ne:H_2 mixtures (Samples 1-6), while in pure H_2 (Sample 7) only a transition similar to transition 1 was observed.

The third ENDOR transition shown in Fig. 7 recovered the right H_{bc} line component (C3) and corresponded to a hyperfine constant change of +5.8(5) MHz. This line was observed previously [18–20] and was associated with H atoms in somewhat cramped substitutional sites of solid Ne. The spectroscopic parameters for pure H_2 (Sample 7) are presented in Table I for comparison.

C. Effect of temperature and helium film on ESR spectra

After storing the samples for 1-3 days to accumulate H atoms produced by tritium decay, we condensed small amounts of helium into the sample cell sufficient to form a superfluid film covering the sample cell walls. The film is required for accumulation and storage of the H and D atoms in the gas phase to be used as the magnetic field markers. We found that the admission of helium had an immediate and remarkable influence on the ESR spectra of all as-deposited samples as described below. Condensing the He film into the sample cell was naturally accompanied by a rise of temperature from 0.1 to 0.6-0.7 K, resulted from the refluxing helium vapor. In order to separate out the effect of sample heating, prior to condensing He, we performed a separate study of the effect of temperature on the properties of the samples in the temperature range from 0.1 K to 0.6 K.

We found that raising the temperature leads to an abrupt decrease of the component C1 of the H ESR spectrum. This effect was somewhat different for the samples with different concentrations of H_2. The strongest drop of the signal (by $\sim$ 70%) was observed for Sample 3 with 1% of H_2 concentration. The effect was very weak for the "pure" neon Sample 1, whereas $\simeq$25% of atoms disappeared in Samples 2 (Ne:0.2% H_2), 4 (Ne:3% H_2) and 5 (Ne:6% H_2).

To get further insight into this phenomenon, we studied the behavior of the C1 intensity in response to a series of step-like increases of temperature by 100-200 mK. The temperature was raised and stabilized with a characteristic time of $\approx$ 30 sec. ESR spectra were recorded with the same time interval. After each step we observed a drop of the C1 intensity which was detected even for the first recorded ESR spectrum, as shown in Fig. 8. The ESR line intensity did not change further until the next step. The total decrease of the C1 intensity after heating to 0.6 K was $\approx$ 70%. In order to better resolve the dynamics

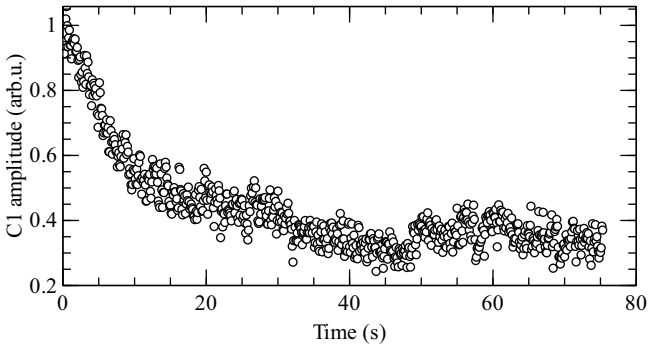

Figure 9. Time evolution of the C1 amplitude in Sample 3 (Ne:1%H_2) after an instantaneous rise of temperature from 0.1 to 0.6 K.

of this effect we applied a heat pulse to the sample cell while standing at the C1 peak maximum and measuring the C1 component amplitude as a function of time after the pulse. We adjusted the energy of the pulse to heat the cell from 0.1 to 0.6 K within several seconds. The evolution of the C1 amplitude after the heat pulse is presented in Fig. 9. The characteristic decay time extracted from such a measurement is $\simeq$10 s. In fact, this decay time is an upper limit estimate of the actual decrease time, since the thermal response time of the sample cell to the heating pulse is of about the same order.

One can see in Fig. 8 that the heating steps did not influence the other components of the H ESR spectrum. We measured the eventual recovery of Component 1 in Sample 3 after destruction by heating to 0.6 K and found that it recovered with the same speed as for its growth before destruction. This leads us to the conclusion that the observed rapid decay is not related to spin-relaxation effects, but is caused by the recombination of atoms.

It should be emphasized that the temperatures 0.3-0.6 K are extremely low, and in our previous work, we were only able to detect a tiny decrease of the ESR signal due to recombination of H atoms in H_2 films on the time scale of several days [32]. Recombination of H atoms on the time scale of seconds provides evidence of an extremely high recombination rate. For the estimate of the rate constant we need to know the local density of the H atoms in the nanoclusters of H_2. Here the main uncertainty comes from the unknown volume of these clusters and distribution of atoms in them. Therefore, the most reasonable estimate of the density can be done from the homogeneous contribution to the C1 line width caused by the dipole-dipole interactions between atoms, which is proportional to the H density $\Delta H_{hom}[G] \approx 0.85 \cdot 10^{-19} n$ [cm^{-3}] [32]. This broadening was measured by burning a hole in the ESR line, which resulted in the hole width of ≈ 0.1 G. Since there can be other mechanisms of the inhomogeneous broadening this provides an upper limit estimate of the H density $n \leq 1.3 \cdot 10^{18}$ cm^{-3}. Then, assuming the second order recombination process $dn/dt = -2k_r n^2$ and using an upper limit estimate for the half-decay time $\tau \leq 10$ s, we obtain a lower limit estimate for the recombination rate constant $k_r \geq 5 \cdot 10^{-20}$ $cm^3 s^{-1}$. This has to be compared with the previously measured recombination rate constant of H atoms in the solid H_2 at the same temperature $k_r \sim (2-10) \cdot 10^{-25}$ $cm^3 s^{-1}$ [32, 33].

In order to study the influence of helium on the sample properties, we stabilized the cell temperature at 0.6 K and He gas was slowly condensed in 2-μmole portions. Condensing helium led to a nearly complete sudden recombination of H atoms corresponding to Component 1 in Samples 1-3 with low concentration of hydrogen. The decrease of the C1 intensity was also observed for Samples 4-5, but the line did not completely disappear in this case. This change of the C1 intensity was irreversible in the sense that no further growth was observed even after pumping out helium from the sample cell and cooling it to 0.1 K.

For Samples 1-3 in addition to the decrease of C1 in the H spectrum we found that a new ESR line (g=2.00234, see Fig. 5) started growing in the spectrum center immediately after admission of helium. This line growth changed to a decrease after pumping out helium from the sample cell, and eventually it vanished in the noise. We conclude that for the low concentration samples 1-3, the presence of helium is necessary to observe the narrow electron line. The situation was different for the samples with a 3% and higher H_2 admixtures, where the same electron line (g=2.00234) appeared immediately after deposition of the samples, and condensing He did not affect its width or amplitude.

Condensing helium into the sample cell with neon films resulted in a significant shift of the quartz microbalance frequency, $\sim$1500 Hz, which was reproducible for all as-deposited samples. It should be emphasized that only non-superfluid He layers deposited on the quartz microbalance can be detected while the superfluid fraction decouples from the QM oscillations and does not contribute to the frequency shift. Thus the saturated superfluid film condensed into the empty cell leads to the QM shift of several Hz corresponding to several normal layers of helium. The QM frequency shift upon condensing He into the cell for "pure" Ne as-deposited Sample 6 (Fig. 10) is the largest for the first 2-μmole He portion ($\sim$450 Hz) and it gradually decreases for the following ones. Condensing the last 2-μmol He portions results only in a minor frequency shift ($<$1 Hz) which allows us to conclude that the process is saturated and all pores are filled by helium. The observed QM frequency shift of 1500 Hz is equivalent to adsorption of $\sim$1100 non-superfluid He monolayers on the Ne film with a thickness of 11000 monolayers.

A large shift of the quartz-microbalance oscillation frequency after condensing helium allows us to suggest a large porosity of the as-deposited neon films. In order to eliminate this and make crystals more regular we performed an annealing procedure. The cell temperature was increased to T=7-10 K for 1.5 hours. The annealing

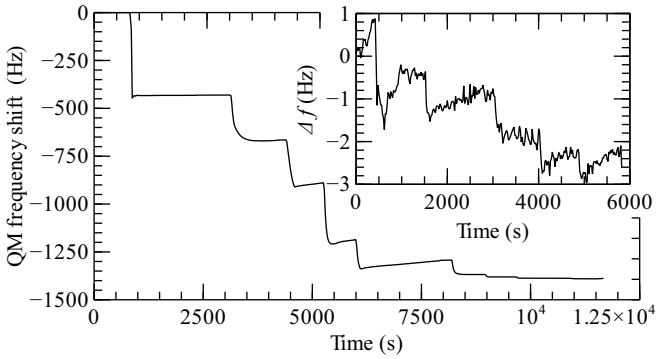

Figure 10. The quartz microbalance frequency shift after condensing helium while storing the as-deposited (main plot) and annealed "pure" Ne Sample 6 (inset). Each step-like quartz-microbalance frequency shift corresponds to a condensation of 2μmol of He into the sample cell.

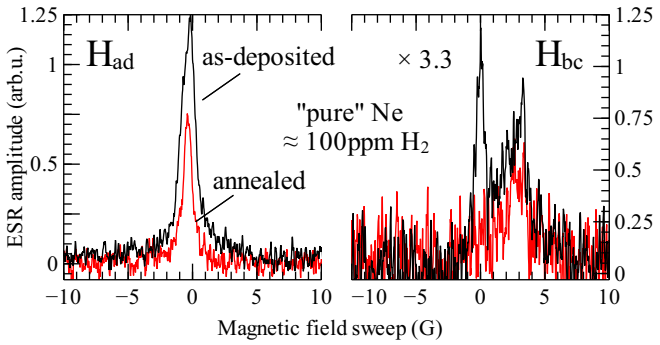

Figure 11. H atom ESR lines measured in "pure" Ne Sample 6 before (black) and after sample annealing (red). Note that the H_{bc} line amplitude is multiplied by a factor of 3.3.

temperatures were chosen to be higher than 1/4 of the Ne melting temperature [34]. This was sufficient for a partial sublimation of the neon film $\sim 10-15\%$ to occur. After annealing, the sample cell was cooled to 0.6 K and the experimental procedure of condensing helium was carried out again. We found that the annealing procedure worked well for samples with the smallest concentration of H_2. The QM frequency shift due to admission of He for the annealed ("pure" neon) Sample 6 was only $\simeq$5 Hz (inset in Fig. 10). We did not observe any film erosion effects caused by electron bombardment [16]. Condensing helium into the cell right after annealing and after storing the annealed samples for 2 days led to the same QM frequency shift (about 5 Hz).

For the samples with larger concentrations of hydrogen, the above described annealing procedure did not work well. The helium-related QM shift decreased by the factor of 3, but still remained at the level of 400-500 Hz, allowing us to assume that substantial porosity remained and could not be removed by the annealing procedure used.

The influence of annealing on the ESR spectrum was

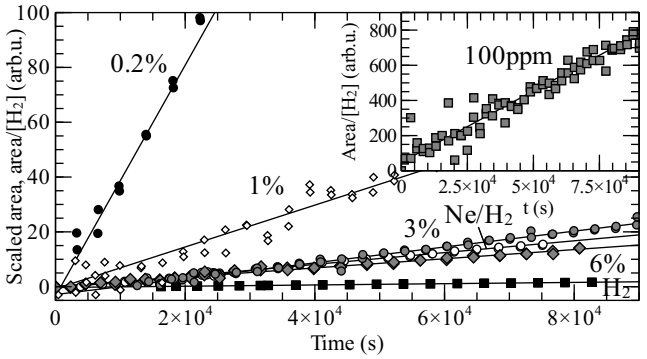

Figure 12. Accumulation rates of H atoms in the samples described in this work. The Y-axis units for each plot are scaled to the estimated number of H_2 molecules in each sample, *i.e.* the ESR line integral/[H_2]. The H_2 admixtures in Ne are labeled near each data set. Ne/H_2 should be understood as a 160 nm H_2 film deposited on top of the annealed neon film (Sample 6). The H_2 admixture in the "pure" neon sample was considered to be 10^{-4} (100ppm).

different for samples with different concentrations. For the "pure" Ne Sample 6 (Fig. 11) no helium was added, and the ESR spectrum contained components 1-3 before annealing. The H ESR lines became narrower after annealing and contained only Component 3. Annealing samples with higher concentrations led to further decrease of the C1 component. We recall that part of it disappeared in recombination after heating and helium admission. All components remained in the spectrum and became more narrow and better resolved.

D. Efficiency of H atom accumulation in solid Ne samples

All as-prepared samples were stored for several days in order to estimate the accumulation rates of H atoms. The flux of electrons resulting from decay of tritium in the sample cell walls was essentially the same for all samples, and the growth rate of the signals represent the efficiency of the dissociation process. We found that the growth rate of the H atom signal in "pure" neon films containing 100 ppm H_2 was only 20 times smaller than that in pure H_2 of the same thickness. Even more striking was the enhancement of the accumulation rate, d[H]/dt, which was observed in Samples 3 and 4 where it matched that in pure hydrogen. In order to compare the efficiency of dissociation we scaled the growth of H atom ESR signals to an estimated number of H_2 molecules in each sample. The ratio of H atom ESR line integrals to H_2 content in the neon-hydrogen films is displayed in Fig. 12. We found that the H atom accumulation efficiency in Ne:H_2 solid mixtures is much larger in comparison to that for pure H_2 samples and it has a tendency to increase when the H_2 admixture in solid Ne decreases.

We considered two possible explanations for a smaller

efficiency of H atom accumulation in solid hydrogen compared to that in solid neon-hydrogen mixtures. The H atoms generated by β-particles in solid H_2 may recombine during thermalization, and the resulting fast recombination might lead to decreasing of their yield. Previously we found out that every β-particle generates about 50 H atoms in a solid H_2 film [27] which is more than an order of magnitude smaller as compared to that observed in the gas-phase [35]. Although the matrix may provide pathways for an excited molecule to relax back to the ground state without being dissociated, it might be considered that a significant number of H atoms in pure H_2 instantaneously recombine back, thus reducing the H atom yield. The second possibility we considered is an enhancement of the accumulation rate in the neon samples due to the action of secondary electrons which significantly amplify production of H atoms. To prove the second mechanism we performed an experiment in which we created a layered Ne/H_2 sample where a 160 nm H_2 layer was deposited on top of the annealed neon film (Sample 6). We found that the accumulation efficiency of H atoms in the H_2 layer deposited on top of a Ne film was nearly 9 times higher as compared to pure H_2 films. The penetration depth of electrons with energy of 5.7 keV into solid H_2, $\simeq$3.5 μm [17], exceeds the thickness of pure hydrogen films we studied which should insure a rather uniform generation of H atoms both in thick, 2.5 μm solid Ne and 160 nm H_2 films. This led us to the conclusion that the enhancement of H atom accumulation efficiency in solid neon-hydrogen films is indeed caused by a large yield of secondary electrons. The enhancement of accumulation efficiency at very low H_2 concentrations in solid Ne, on the other hand, provides evidence for a suppression of atomic hydrogen recombination under these conditions.

IV. DISCUSSION

In this work we report observations and measurements of the main spectroscopic parameters for the three doublets of H atoms in the ESR spectra. The values of these parameters are in good agreement with previous studies [2, 18, 19] (see Table I). Dmitriev et al. [19] observed the H atom ESR doublets characterized by both positive and negative hyperfine constant shifts in their Ne:H_2 samples created by co-deposition of the rf-discharge products at small H_2 concentrations (10-100 ppm) at T=4.2 K. The spectroscopic parameters obtained in their work appeared to be similar to Components 3 and 2, respectively, in our experiments. The spectroscopic parameters of H atoms in solid Ne described in refs. [2, 18] are presented in Table I. They are nearly same as reported here.

The ENDOR transitions provide information on the change of the hyperfine constant, which is most sensitive to the environment of impurity atoms and allows characterization of their position in the solid neon-hydrogen matrix. The characterizations which we consider below are in good agreement with conclusions made in the previous studies [2, 18, 19].

Component 1 has a negative hyperfine constant change, $\Delta A = -2.6(4)$ MHz, A=1417.8(4) MHz. This is somewhat smaller than the hyperfine constant change for H atoms in a pure H_2 environment $\Delta A = -3.0(2)$ MHz. We suggest that the small reduction of ΔA may be caused by a presence of both H_2 molecules and Ne atoms in the closest neighborhood of H atoms. We assign the C1 component to the hydrogen atoms trapped in pure H_2 regions, clusters or micro-crystals embedded in the neon matrix.

The polarizability of Ne atoms is even smaller than that of H_2 molecules which should result in a smaller hyperfine constant change. Therefore, we suggest that Component 2, characterized by ΔA=-1.4(3) MHz, A=1419.0(3) MHz, is related to H atoms in the substitutional sites of the Ne lattice.

The third component C3 is characterized by a clearly positive hyperfine constant change, ΔA=5.8(5) MHz, A=1426.2(5) MHz. Even though the shift is positive, its absolute value is too small for the pure interstitial position. It might be expected that the extremely small polarizability of Ne atoms will lead to a dominance of the Pauli repulsion even at long distances. Therefore, we attribute the C3 component to H atoms, which were initially stabilized in octahedral interstitial voids of the Ne lattice, then relaxed to a position which is somewhat intermediate between a substitutional and a more cramped octahedral interstitial one, as was suggested theoretically by Kiljunen et al. [15].

From the previous studies it is known that H atoms can occupy different lattice sites depending on the substrate temperature and deposition rate. Vaskonen et al. [36] observed two ESR line doublets of H atoms in solid Ar and Kr and associated them with H atoms in substitutional and octahedral interstitial sites, respectively. The doublet assigned to the substitutional sites of H atoms in solid Ar and Kr appeared stronger for colder substrates and higher deposition rates, conditions which favor formation of vacancies. Annealing the sample decreases the number of vacancies and more atoms become trapped in the octahedral interstitial sites. A similar result was observed in our work where only Component 3 remained after annealing a "pure" Ne sample.

The new and unexpected observation is the strong influence of temperature and the superfluid helium film on the properties of atoms trapped in clusters of the pure H_2 (C1 component), which we first summarize and then try to explain below.

Raising the temperature over the range 0.1-0.6 K leads to a rapid recombination of the fraction of the H atoms corresponding to the C1 component. The rest of these atoms remain stable until a further temperature increase is performed. The effect is strongest for the 1% concentration, where 2/3 of the C1 component is destroyed by raising the temperature from 0.1 to 0.6 K. The recombination is very fast and occurs on the time scale

comparable with the thermal response of the sample cell to the heating pulse. We evaluated the lower limit for the recombination rate constant $k_r \geq 5 \cdot 10^{-20}$ cm^{3}s^{-1}, to be nearly five orders of magnitude larger than that measured previously in pure H_2 films [32]. Lowering the temperature back to 0.1 K leads to a recovery of the C1 component with the same accumulation rate observed during initial H atom accumulation in this sample due to the tritium decay. Admission of a helium film completely destroys the C1 component in the samples with small concentrations of hydrogen ($\leq 1\%$). The destruction is irreversible: pumping out helium and cooling back to 0.1 K does not lead to the growth of the C1 component. For higher concentrations of H_2 in Ne the destruction by admission of helium is only partial, with most of the C1 atoms surviving. Annealing of the samples leads to the complete disappearance of the C1 component at small concentrations ($\leq 1\%$ samples 1-3), while for larger concentration (samples 4,5) part of the C1 line survives the annealing procedure.

The very fast changes which occur with the hydrogen atoms trapped in the pure H_2 regions upon heating, motivates us to consider a possible phase transition as the main effect behind the observed behavior.

First we consider possible phases of hydrogen in neon. Gal'tsov et al. [1] showed that solid Ne:H_2 mixtures with 2-12% H_2 admixtures are characterized by a co-existence of the *fcc* and *hcp* phases of solid neon with nearly identical lattice parameters. The latter phase is rich in H_2 and appears stable up to about 16 K, while the former may accommodate not more than $\simeq$2% H_2 without being driven out of equilibrium and transforming to the *hcp* phase which is able to store larger amounts of H_2. It might be suggested that the C1 component we observe corresponds to H atoms in the regions rich in molecular hydrogen corresponding to a highly unstable *fcc* lattice. This phase might be stabilized by defects whereas raising the temperature or condensing helium might trigger the phase transition. One might expect that the possible transition of the unstable hydrogen-rich *fcc* neon lattice to the more stable *hcp* phase should be irreversible and appear only once. However, the C1 component recovered on a time scale of hours if the cell temperature was returned to 0.1 K and atomic recombination could be triggered again by raising the temperature to 0.3-0.6 K. A fast recombination such as we observed cannot appear in any solid matrix, irrespective of its type. On this basis we concluded that the above described behavior is not related to the *fcc* - *hcp* phase transition in Ne:H_2 solid mixtures.

The other possibility for explaining the rapid recombination of H atoms upon raising the temperature is the solid-to-liquid transition in H_2 clusters. Clearly, if the H atoms were in the liquid, they would have a very high mobility, which could explain the fast recombination of C1 component. It is known that for molecular hydrogen in a restricted geometry, the solidification temperature may be substantially reduced. This is confirmed in experiments in porous media [37–39]. The liquid behavior of small hydrogen clusters ($\sim 10^4$ molecules) in helium nanodroplets has been observed in the experiments of Kuyanov-Prozument and Vilesov [5] at temperatures ~ 2 K. Theoretical calculations predict liquid and even superfluid behavior for small (≤ 30 molecules) clusters of H_2 at temperatures below 1 K [6–8], while for large size of clusters no such prediction exists. The superfluid behavior had a possible experimental confirmation in the experiments of Grebenev *et. al.* [9], but has been under discussion by other authors [10, 11].

In our samples the phases of pure H_2 are definitely formed, and are associated with the C1 component of the H atom ESR line. We may assume that these phases form clusters of H_2 molecules of different sizes with a distribution around the mean value. The average size should depend on the concentration of molecular hydrogen in the condensed neon-hydrogen mixture. Once we observe strong porosity of as-deposited films, it is natural to suggest that all H_2 clusters or at least part of them are located in the pores of the Ne matrix. With these assumptions we arrive at a system with small hydrogen clusters in a confined geometry where a solid-to-liquid transition may occur at very low temperatures. The H_2 clusters accumulate atomic hydrogen after dissociation enhanced by secondary electrons. We note that the estimated concentration of atoms $n \leq 10^{18}$ cm^{-3} corresponds to one atom per 10^4 molecules or less, and therefore the size of the clusters accommodating several H atoms should be substantially larger than that. The solid-liquid transition temperature should depend on the size of the cluster. Therefore, by raising the sample temperature, we trigger the solid-liquid transition in a fraction of them having the proper size. The atoms inside these clusters acquire a high mobility inside the liquid and rapidly recombine, while the others, remaining solid, keep their atoms stabilized in the H_2 matrix. A subsequent heating step involves another fraction of the clusters, and so on. Cooling back to 0.1 K transfers them back to the solid state, and accumulation of atoms starts with the same rate. For high concentrations of hydrogen the average size is shifted towards very large clusters, which remain solid in the whole temperature range of experiment. That is why for the samples 4-5 the fraction of recombined atoms upon heating is smaller. It seems that the sample with 1% concentration of H_2 has the average size of clusters which best matches the solid-to-liquid transition in the studied temperature range 0.1-0.6 K, which explains why the effect is strongest for this sample.

When we condense helium, it diffuses into the pores and voids of the sample, and is collected at the boundary between the H_2 clusters and the neon crystal. This changes the boundary conditions, and should obviously change the solid-to-liquid transition temperature. It may trigger this transition for a fraction of the clusters without any extra heating. It is also known that pumping out helium will never remove it all from the system. One or two monolayers will remain adsorbed on the surface,

and the first one may be even in the solid state. Therefore, once condensed, helium makes a permanent change of the state for part of the clusters. For small concentrations of H_2 the average cluster size is such that most of these clusters remain liquid below 1 K and no hydrogen atoms may be accumulated in them. Another feature of helium which may play important role at the boundary of the clusters is that it effectively slows down electrons [40, 41], which may enhance their trapping inside the clusters. This is indeed observed in our experiments by the growth of the narrow component of the singlet line associated with electrons trapped inside H_2. For larger H_2-Ne concentrations we get a larger fraction of very large clusters which always remain solid and contain H atoms with the C1 component. Annealing seems to reduce the number of C1 atoms in the large clusters because of recombination, but probably does not influence the state of the large clusters. Helium atoms may still reside at the boundaries between the clusters and the neon lattice, which have fairly large areas for large H_2 concentrations. This explains why relatively large amounts of helium may be still absorbed by the Samples 3-4 even after annealing. Therefore, all observed effects during warming samples from 0.1 to 0.6 K and additions of liquid ^{4}He can be explained by a solid-liquid phase transition in H_2 clusters.

Another new observation is the enhancement of the accumulation rate of H atoms in neon samples which appeared to be nearly two orders of magnitude larger compared to that in pure H_2 films of the same thickness. The accumulation rate enhancement was also observed for H atoms in a H_2 layer deposited on top of the annealed Ne film. We suggest that this is related to secondary electrons generated in solid Ne by β-particles released in the tritium decay. This agrees qualitatively with the yield of secondary electrons in solid neon exposed to up to 3 keV primary electrons, $\simeq$70, reported by Bozhko et al. [42]. The accumulation efficiency in dilute Ne:H_2 mixtures decreased at higher H_2 concentrations which might be related to a higher recombination rate of H atoms in large clusters of pure H_2. Similar behavior was observed for photolysis of HBr in solid Ar, where the HBr dissociation efficiency estimated from the atomic hydrogen yield increased from 18% for a 1:500 matrix to 100% in a 1:8000 matrix [43].

V. CONCLUSIONS

We have reported on the ESR study of H atoms stabilized in a solid neon matrix carried out in a high magnetic field of 4.6 T and at temperatures below 1 K. The H atoms were generated *in situ* by electrons released during decay of tritium trapped in the walls of our sample cell. The ESR lines of H atoms had a complex structure which was associated with their three different locations: two in the substitutional positions of neon and the third one in clusters of pure H_2.

It was also found that the accumulation of H atoms in Ne:H_2 solid mixtures is greatly enhanced by the secondary electrons released from neon atoms upon their bombardment by $\beta-$particles generated in tritium decay. The accumulation efficiency is even more enhanced for samples with smaller H_2 admixtures in solid Ne where H atom recombination appears to be less efficient compared to samples with a higher H_2 abundance. This result may have important applications for creation of high densities of free radicals in solid matrices

We observed peculiar behavior of the H atoms trapped inside pure molecular hydrogen clusters located in pores of the neon matrix. Heating in the temperature range 0.1-0.6 K triggered abrupt recombination of trapped hydrogen atoms. Such rapid recombination cannot occur in solids, where the recombination process is limited by the slow diffusion of atoms. We suggest that this effect occurs due to a solid-to-liquid transition in H_2 clusters of certain sizes. This may be one more piece of evidence for the elusive liquid state of H_2 in a restricted geometry at ultra-low temperatures. A possible search for a superfluidity in these clusters could be an intriguing continuation of this research work.

ACKNOWLEDGMENTS

We acknowledge funding from the Wihuri Foundation and the Academy of Finland grants No. 258074, 260531 and 268745. This work is also supported by US NSF grant No DMR 1707565. S.S. thanks UTUGS and the Turku University Foundation for support.

[1] N. N. Gal'tsov, A. I. Prokhvatilov, and M. A. Strzhemechnyi, Low Temperature Physics **30**, 984 (2004).
[2] R. A. Zhitnikov and Y. A. Dmitriev, JETP **65**, 1075 (1987).
[3] W. Schulze and D. M. Kolb, Journal of the Chemical Society, Faraday Transactions 2: Molecular and Chemical Physics **70**, 1098 (1974).
[4] V. L. Ginzburg and A. A. Sobyanin, JETP Letters **15**, 242 (1972).
[5] K. Kuyanov-Prozument and A. F. Vilesov, Phys. Rev. Lett. **101**, 205301 (2008).
[6] P. Sindzingre, D. M. Ceperley, and M. L. Klein, Phys. Rev. Lett. **67**, 1871 (1991).
[7] Y. Kwon and K. B. Whaley, Phys. Rev. Lett. **89**, 273401 (2002).
[8] F. Mezzacapo and M. Boninsegni, Phys. Rev. Lett. **97**, 045301 (2006).
[9] S. Grebenev, B. Sartakov, J. P. Toennies, and A. F.

Vilesov, Science **289**, 1532 (2000).
[10] C. Callegari, K. K. Lehmann, R. Schmied, and G. Scoles, The Journal of Chemical Physics **115**, 10090 (2001).
[11] T. Omiyinka and M. Boninsegni, Phys. Rev. B **90**, 064511 (2014).
[12] F. J. Adrian, The Journal of Chemical Physics **32**, 972 (1960).
[13] G. L. Hall, Journal of Physics and Chemistry of Solids **3**, 210 (1957).
[14] D. Li and G. A. Voth, J. Chem. Phys. **100**, 1785 (1994).
[15] T. Kiljunen, J. Eloranta, and H. Kunttu, The Journal of Chemical Physics **110**, 11814 (1999).
[16] J. Schou, P. Børgesen, O. Ellegaard, H. Sørensen, and C. Claussen, Phys. Rev. B **34**, 93 (1986).
[17] J. Schou and H. Sørensen, Journal of Applied Physics **49**, 816 (1978).
[18] S. N. Foner, E. L. Cochran, V. A. Bowers, and C. K. Jen, The Journal of Chemical Physics **32**, 963 (1960).
[19] Y. A. Dmitriev, R. A. Zhytnikov, and M. Kaimakov, Fizika Nizkikh Temperatur **15**, 495 (1989).
[20] L. B. Knight Jr., W. E. Rice, L. Moore, E. R. Davidson, and R. S. Dailey, J. Chem. Phys. **109**, 1409 (1998).
[21] M. D. Correnti, K. P. Dickert, M. A. Pittman, J. W. Felmly, J. J. I. Banisaukas, and L. B. Knight Jr., J. Chem. Phys. **137**, 204308 (2012).
[22] S. Sheludiakov, J. Ahokas, O. Vainio, J. Järvinen, D. Zvezdov, S. Vasiliev, V. V. Khmelenko, S. Mao, and D. M. Lee, Rev. Sci. Instrum. **85**, 053902 (2014).
[23] S. Vasilyev, J. Jarvinen, E. Tjukanoff, A. Kharitonov, and S. Jaakkola, Rev. Sci. Instrum. **75**, 94 (2004).
[24] G. Feher, Phys. Rev. **103**, 834 (1956).
[25] R. van Roijen, J. Berkhout, B. Hebral, and J. Walraven, "A cryogenic dissociator for atomic hydrogen," unpublished.
[26] J. Helffrich, M. Maley, M. Krusius, and J. C. Wheatley, Journal of Low Temperature Physics **66**, 277 (1987).
[27] S. Sheludiakov, J. Ahokas, J. Järvinen, L. Lehtonen, O. Vainio, S. Vasiliev, D. M. Lee, and V. V. Khmelenko, Phys. Chem. Chem. Phys. **19**, 2834 (2017).
[28] G. W. Collins, P. C. Souers, F. Magnotta, E. R. Mapoles, and J. R. Gaines, Phys. Rev. B **53**, 8143 (1996).
[29] S. Sheludiakov, J. Ahokas, J. Järvinen, O. Vainio, L. Lehtonen, D. Zvezdov, V. Khmelenko, D. M. Lee, and S. Vasiliev, Journal of Low Temperature Physics **183**, 120 (2015).
[30] J. Vanier and C. Audoin, *The quantum physics of atomic frequency standards*, The Quantum Physics of Atomic Frequency Standards No. v. 2 (A. Hilger, 1989).
[31] S. Sheludiakov, J. Ahokas, J. Järvinen, D. Zvezdov, O. Vainio, L. Lehtonen, S. Vasiliev, S. Mao, V. V. Khmelenko, and D. M. Lee, Phys. Rev. Lett. **113**, 265303 (2014).
[32] J. Ahokas, O. Vainio, S. Novotny, J. Järvinen, V. V. Khmelenko, D. M. Lee, and S. Vasiliev, Phys. Rev. B **81**, 104516 (2010).
[33] J. Ahokas, J. Järvinen, V. V. Khmelenko, D. M. Lee, and S. Vasiliev, Phys. Rev. Lett. **97**, 095301 (2006).
[34] S. A. Nepijko, I. Rabin, and W. Schulze, ChemPhysChem **6**, 235 (2005).
[35] G. W. Collins, P. C. Souers, J. L. Maienschein, E. R. Mapoles, and J. R. Gaines, Phys. Rev. B **45**, 549 (1992).
[36] K. Vaskonen, J. Eloranta, T. Kiljunen, and H. Kunttu, The Journal of Chemical Physics **110**, 2122 (1999).
[37] J. L. Tell and H. J. Maris, Phys. Rev. B **28**, 5122 (1983).
[38] E. Molz, A. P. Y. Wong, M. H. W. Chan, and J. R. Beamish, Phys. Rev. B **48**, 5741 (1993).
[39] P. E. Sokol, R. T. Azuah, M. R. Gibbs, and S. M. Bennington, Journal of Low Temperature Physics **103**, 23 (1996).
[40] Y. A. Dmitriev, Journal of Low Temperature Physics **150**, 544 (2008).
[41] Y. A. Dmitriev, Journal of Low Temperature Physics **158**, 502 (2009).
[42] Y. Bozhko, J. Barnard, and N. Hilleret, arXiv:1302.2334v1 (2013).
[43] J. Eloranta, K. Vaskonen, and H. Kunttu, The Journal of Chemical Physics **110**, 7917 (1999).